International Journal of Advanced Research in Physical Science (IJARPS)
Volume 7, Issue 2, 2020, PP 1-15
ISSN No. (Online) 2349-7882
www.arcjournals.org

Some Problems of Modeling Laser-Induced Filaments: Nonlinear and Relaxed Optical Aspects

Petro P. Trokhimchuck*

Anatoliy Svidzinskiy Department of Theoretical and Mathematical Physics, Lesya Ukrayinka Eastern European NationalUniversity, Ukraine.

Corresponding Author:** ***Petro P. Trokhimchuck, *Anatoliy Svidzinskiy Department of Theoretical and Mathematical Physics, Lesya Ukrayinka Eastern European National University, Ukraine.*

Abstract: *Experimental data of formation laser-induced filaments in various matter are represented. These phenomena are represented as processes of Relaxed Optics. Problems of modeling the creation the volume laser-induced filaments are observed. Comparative analysis of plasmic, nonlinear optical, diffractive and interference phenomena (including diffractive stratification), shocking processes (including Cherenkov radiation) and physical-chemical processes (cascade model of excitation the proper chemical bonds in the regime of saturation the excitation) methods and models are represented and discussed. These methods were used for modeling the processes of creation volume laser-induced structures in various matter. Modified Rayleygh models, modified I. Frank and N. and A. Bohrs models and cascade model explanation these experimental data is fuller and really as other models. These models allow to explain oe represented experimental data.*

Keywords: *laser irradiation, filaments, Rayleygh, Bohr, Frank, Cherenkov radiation, diffractive stratification, Relaxed Optics.*

1. INTRODUCTION

Problems of modeling the creation the volume laser-induced structures (filaments) are very interesting [1 – 5]. These structures have various sizes: from nanometetrs in solid [6, 7] to few hundred meters in air [8 – 12]. In whole, we can have various processes and phenomena, which are connected with photochemical, plasmic and thermochemical processes [2 – 5, 13, 14]. It may be various processes, including the cascade and circle processes. Irreversible changes of laser-irradiated volume of matter must be explained as phase transformations. These processes have shock nature and connected with multiphoton scattering processes [15, 16].

First filaments were observed in 1965 after 20 MW nanopulse laser irradiation of organic liquid (toluol, cyclohexane, ortoxylene, CCl_4) [17]. These processes are connected with self-focusing processes. Self-focusing of light radiation in air is observed for the convergent and collimated beams.

The self-focusing is the complex process and included various physical phenomena. Among them are conic radiation (emission), diffractive stratification, generation of optical-induced Chertenkov radiation and phase transformations in solid [3 – 7, 18 – 25].

We selected basic experimental data, which are allow to select basic peculiarities of processes the laser-induced filamentation in various media from air to silicon carbide.

The basic results are explained with point of view of transformation of initial radiation in other types of irradiation. It is essentially nonlinear optical processes. But trace of finished result of this interaction in irradiated matter is little-studied. It may be nonequilibrium processes for the liquid and gas and irreversible processes for the solid. The question of transition from nonequilibrium to irreversible process is little-studied for these phenomena. Therefore we use methods and results of Nonlinear and Relaxed Optics for the resolution of this problem. Electrodynamics methods were united with physical-chemical methods for the explanation of the chain basic processes, which are allowed to model represented experimental data.

We shown and created theories and methods, which are can explain all represented experimental data. Among them modified Rayleygh theory of diffractive rings of diffractive stratification of laser beam,

Lugovoy – Prokhorov theory of moving focuses [26], physical-chemical method of estimation the threshold energies for proper chain process, modified Rayleygh model of estimation the sizes the nanoneeds, continuum mechanical model for the determination the forms and sizes of laser-induced nanovoids, modified I. Frank model of interference the Cherenkov radiation [2 – 4]

Therefore the basic object of this paper is presentation the problem of formation self-focusing and evolution of its trace in the volume of irradiated matter: beginning from diffractive stratification and ending of destruction of solid with point of Relaxed Optics.

2. EXPERIMENTAL DATA

Now we represent principal experimental data, which allow determine main peculiarities of laser-induced generation of filaments.

Laser-induced superbroadening of s pectra were observed in [9, 27]. Later this phenomenon was called supercontinuum [18]. Supercontinuum radiation is conic part of self-focusing [8].

First filaments were observed in 1965 after 20 MW nanopulse laser irradiation of organic liquid (toluol, cyclohexane, ortoxylene, CCl4) [17]. One filament was generated after irradiation of cyclohexane and two filaments for ortoxylene [17]. Focusing region had dumbbell form, filaments were creatyed in the tnd of focusing area and were oriented parallel to laser beam direction.

On Fig. 1 experimental data, which are received for sodium containing heat-pipe with 20 cm active length and a Hänsh-type 10 kW peak dye laser, are represented. The sodium density was 1014 – 1016 cm-3. The beam of 0,5 cm-1 bandwigth laser was focused by a lens into the sodium cell after special filtering. The laser intensity at the focus was 10 MW/cm2 and is sufficient for the formation of self-trapped filaments. The forward emission was photographed by an Alphax B216 camera with f/number of 1,9, placed aft6er the sodium cell without any imaging optics [19]. The laser beam was blocked with small on axis disc to prevent over-expose.

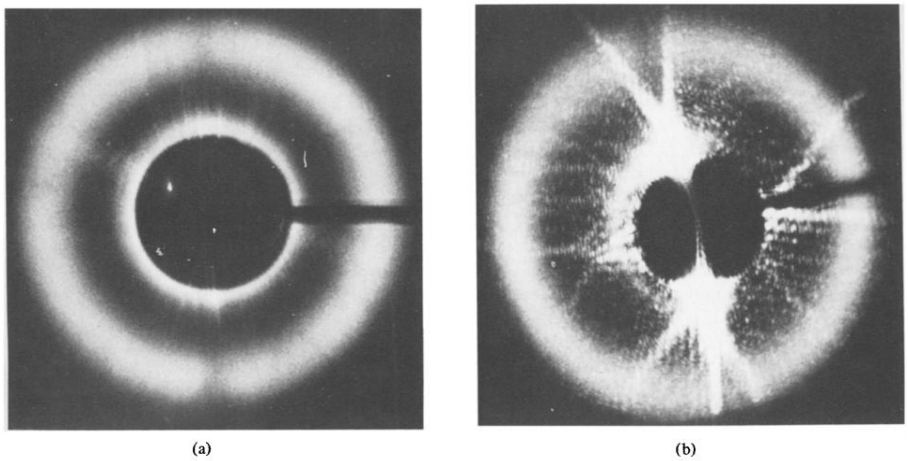

Fig1. *The pattern of the conical radiation at sodium density 1,8·10^{15} cm^{-3} and laser detuning of 0,2 nm to the blue of the D_2 transition. The laser radiation is focused into the sodium cell bay a spherical lens (a) and by a cylindrical lens (b). The laser beam is blocked with a small of on-axis disc. The focal Lin of the cylindrical lens (b) is the long of horizontal line [19].*

The spectral and angular properties of the conical radiation are well-known [19]. The cone angle is 1 - 3º and increases as the laser frequency approaches the atomic transition and with insreasing sodium density. The cone spectrum is broad (5 – 10 cm-1) and is to the red of the transition. For small laser detunings (5 – 10 cm-1) the peak of conic emission is detuning. For large laser detunings (6 – 20 cm-1) the peak detuning exhibits saturation behaviour; the limiting value is at thev dispersionless point – 589,4 nm [19].

Two kinds of experiments were performed to establish the surface character of the conical emission. The light changes polarization of initial beam in a linear case, with a direction determines the difference of right and left polarizations. Self-trapping of laser light close to the transition is due to saturation effects, and this change in polarization is expected to occur inside the filaments, where saturation degree is maximum. In [19] next conclusion was made: conical radiation is generated at a nonsaturated region such as self-trapped filament surface.

The question about spatial coherence of conical radiation was observed in [19]. It was found that the angular and spectral distribution of the conical radiation is independent of lens type. The next conclusion was made the conical radiation from various filaments add upp incoherently and display no interference pattern.

The data of laser irradiated different 1 – 10 cm – long cells containing H2O or D2O are represented in Fig.2 [18]. In these experiments a Quantel YG-471 mode-locked laser was used, which produced 22-psec-duration pulses at 1,06 μm of aup to 35 mJ energy or its second harmonic 15-psec-duration pulses of 12 mJ energy. A variefy of lenses with focal lengths from 2 to 25 cm, capable of producing intensities in the focal spot of up to 1012 W/cm2. Several (usually 5 to 10) filaments were produced by each pulse/ It was easier to produce supercontinuum by focusing the laser beam with long-focal-length lenses into the long cells, and the threshold for supercontinuum in D2O was lower than that in H2O. The supercontinuum was spread in a circular reinbow, and for 1,06-μm excitation the generated photon energy increases with the off-axis angle, while for 0,53-μm excitation the pattern is more complicated.

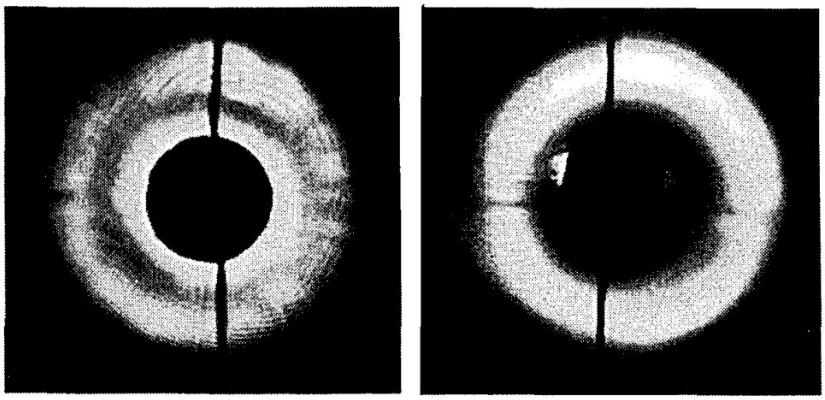

Fig2. *Supercontinuum generated in D_2O by 0,53-μm laser excitation. The laser is focused into the cell (a) by a spherical lens or (b) by a combination the spherical and cylindrical lenses. The laser beam is blocked with a small of on-axis disc. The focal line of the cylindrical lens (b) is the long of vertical line [18].*

Data of Fig. 2 shown that spatial pattern of the supercontinuum conic radiation is independent of the focusing mode, leading one to conclude that the origin of this emission is at the surface of the filaments.

The possibility of generation the Cherenkov radiation in Kerr media was observed in [28]. An influence of velocity the motion of self-focusing focus point and self-modulation on frequency-angle spectra of radiation the parametric anti-Stoke component of Brillouin scattering [28]. The possibility of generation Cherenkov radiation in this case was proved.

The white-light continuum spectra for various media are represented in Fig. 3 [20]. Ti:sapphire laser system based on the chirped-pulse amplification technique produced a 1-mJ, 70-fs pulse at 10-Hz repetition rate. The center wavelength was 785 nm, and the bandwidth was 20 nm. This fundamental pulse, which had a diameter of 7 nm, was converted into second- and third-harmonic pulses by doubling and tripling with two 100-μm-thick β-barium borate crystals. The maximum output energies the second- and third-harmonic pulses were 180 and 30 μJ, respectively.

Comparison of Medium Length and Self-Focusing Length at 400 nm in various materials for two incident intensities was made in [20] and represented in Table 1.

Table1. *Comparison of Medium Length and Self-Focusing Length at 400 nm in various materials for two incident intensities*

Medium	Length (mm)	$n_2, \times 10^{-16}$ W/cm^2	Self-focusing length (mm)	
			$1{,}5 \times 10^{12}$ W/cm^2	1×10^{13} W/cm^2
LiF	1,5	0,98	3,0	0,90
CaF_2	2	1,24	2,1	0,67
Fused silica	2	3,25	1,3	0,46
Water	5	4,1	1,0	0,36
BK7	1	3,78	1,0	0,35

Remark to Table 1 nonlinear refractive indices n2 are also listed [20].

Fig. 3 shows typical white-light continuum spectra of various materials obtained with 393-nm radiation focused at intensity of 1,5·1012 W/cm2.

The bandgaps of the materials, which are represented in Fig. 4 are equaled 4.7, 7.5, 7.5, 10.2 and 11.8 eV for BK7 glass, water, fused silica, CaF2 and LiF, respectively. The pump beam was focused at the front surface of the medium, which was a geometrical focal plane. When the pump laser intensity was gradually increased, the spectral width abruptly increased at a threshold intensity and saturated rapidly. As shown in Fig. 3, large-bandgap materials such as CaF2 and LiF tend to show asymmetric broadening in that the spectrum in the anti-Stokes side broadens much more than that in the Stokes side.

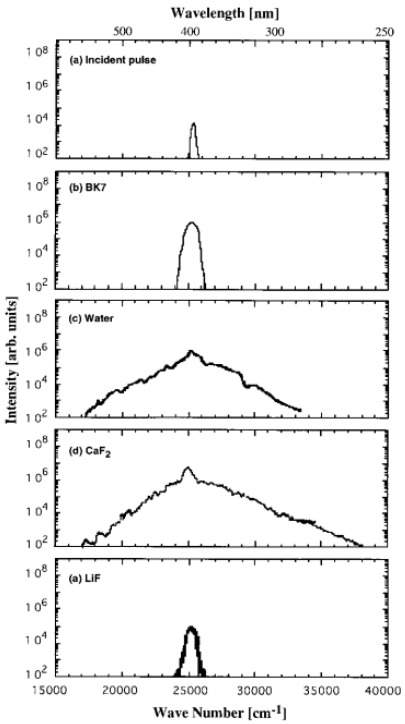

Fig3. *White-light continuum spectra for various media. The insight pump wavelength and intensity are 393 nm and 1.5·10[12] W/cm[2], respectively [20].*

Band-gap dependence of the ultrafast white-light continuum was observed in [29]. A Ti:sapphire laser system is used to generate 140-fs transform-limited pulses centered at λ0=796 nm, with beam diameter 2,2 mm (1/e2 of intensity). The beam is focused with lens into the solid or liquid (contained in stainless-steel cell equipped with two 3-mm fused silica windows), where is propagated vertically upward. The media listed in Table 2 are investigated.

Table2[29]. *Anti-Stokes brodeaning* $\Delta\omega_+$ *and self-focal characteristic measured at power P=1,1*P_{th}*: minimum beam diameter* d_{min} $(\pm 0{,}5\mu m)$, *maximum fluence* F_{max} $(\pm 10\%)$, *and energy loss* E_{loss} $(\pm 1\%)$. P_{th} *is accurate within* ±20%.

Medium	E_{gap} (eV)	$\Delta\omega_+ \left(cm^{-1}\right)$	d_{min} (μm)	F_{max} (J/cm^2)	E_{loss} (%)	P_{th} (MW)
LiF	11,8	19800	10,8	1,3	13	8,8
CaF_2	10,2	18300	10,4	1,0	11	7,4
Water	7,5	14600	9,8	0,62	4	4,4
D_2O	7,5	14600	10,6	0,46	4	3,6
Fused silica	7,5	13500	10,4	0,57	3	4,3
Propanol	6,2	14200	9,1	0,57	3	3,3
Methanol	6,2	14500	10,2	0,54	4	3,9
NaCl	6,2	9000	9,9	0,29	3	2,0
1,4-Dioxane	6,0	10200	9,3	0,44	3	2,7
Chloroform	5,2	11200	10,0	0,29	1	2,2

CCl_4	4,8	10400	8,7	0,44	2	2,5
C_2HCl_3	4,7	950	14,6	0,08	<1	1,2
Benzene	4,5	600	14,0	0,07	<1	0,90
CS_2	3,3	400	15,6	0,01	<1	0,23
SF-11 Glass	3,3	340	15,6	0,03	3	0,52

Comparative analysis of data of Fig. 3 and Table 2 and Fig. 4 (a, b) [29] give various values for LiF and equivalent result for glasses. Continuum spectra for LiF generated from 300 nm to 600 nm, for NaCl – from 450 to 600 nm and for water from 300 to 900 nm.

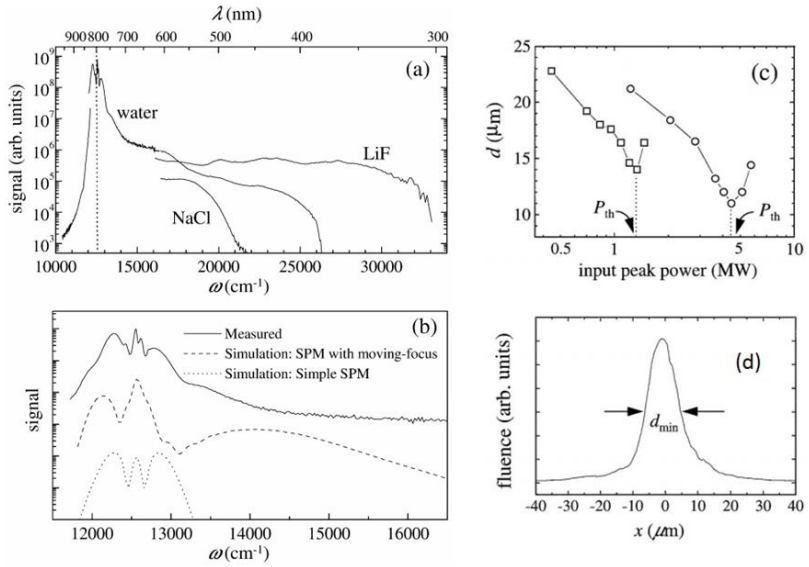

Fig4. *(a) White-light continuum spectrum generated in water, LiF and NaCl at P=1,1P_{th}. Only λ < 630 nm is shown for LiF and NaCl for clarify. (b) Continuum spectra generated in water at P=1,1P_{th} in the experiment (solid line), in 1D simulation including the moving focus dynamics under multiphoton excitation conditions (dashed line) and in simple self-phase modulation (dotted line). (c) Beam diameter d at the geometrical focus, as a function of input peak power. Squares C_2HCl_3 (trichloroethylene); circles^ water. (d) Beam profile with diameter d_{min} at P=P_{th} in water. The sizes d are depending from power of irradiation. At low power d = 27 μm in all media. With increasing power d decreases, reaches a minimum d_{min} at the threshold power P_{th} and then increases. P_{th}, which is defined as the peak power at the entrance of the medium, corresponds to the vertical power for the self-focusing.*

The laser-induced filamentation were received in air after irradiation by femtosecond laser pulses (wavelength 800 nm, pulse duration 85 fs, energy 230 mJ and peak power 2,3 TW, i.e. about 700 critical powers according to [30]) (Fig. 5).

A ring-shape zone supports major spots initiated by the highest intense defects of the initial beam (depth z = 30 m). These "hot" spots self-focus more and more over several meters, while they excite secondary smaller-scaled filaments in their vicinity (z = 35 m) [30]. Evacuation of power excess undergone by the primary filaments finally allows transfer of power to the central zone of the beam, which serves as an energy reservoir for exciting new sequences of small spots (z = 50 m). Numerical data were represented for duration of pulse 85 fs and power few terawatt [30]. From these results specific geometrical zones in the beam pattern were selected [30].

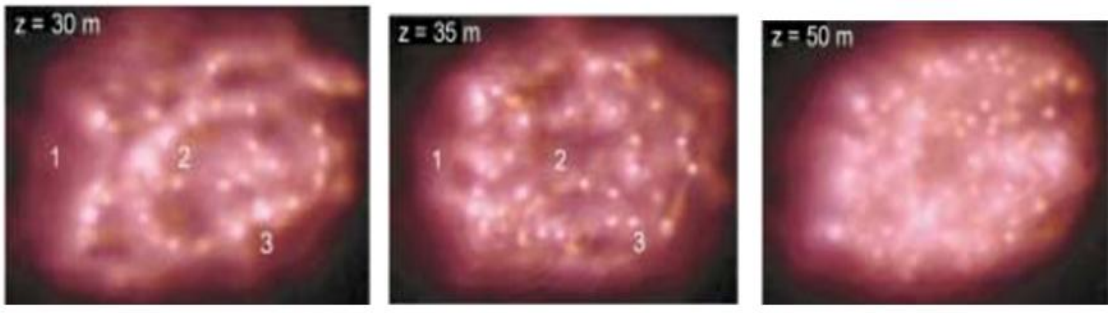

Fig5. *Filamentation pattern of the 700 P_{cr} beam delivered by Teramobile laser. Labels 1-3 spot specific beam zones commented on in the text [30].*

Characteristics examples are indicated by labels 1-3 [Berge]:

- points to a couple of hot couples surviving at further distances;
- indicates in active region of the beam, where intense filaments decay into cell of lesser intensity;
- identifies an area including a cross-wise structure that keeps some filaments robust over 5 m.

Condition of receiving self-focusing is next: self-focusing must be more as diffraction [2].

The time-resolved refractive index and absorption mapping of light-plasma filaments in water were observed in [22].

Refractive index map for two times, which was measured in [22], is represented on Fig. 6.

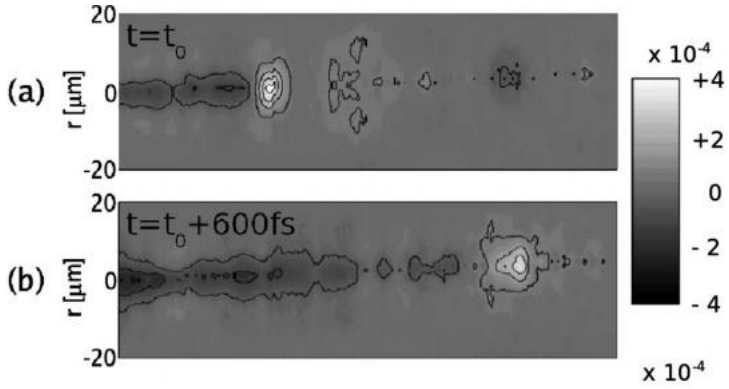

Fig6. *(a) and (b). Refractive index map of the filament taken at two different times and showing the formation of the plasma channel. Horizontal scale: propagation axis ranging from 9,41 mm (left) to 9,68 mm (right) from the input window.*

In contrast to the formation. of surface periodical structures three-dimensional periodic structures were obtained in this case. Sectional area of these structures was ~ 22 μm, the depth of ~ 50 μm. As seen from Fig. 7 (c) we have five stages disordered regions, which are located at a distance from 2 to 4 μm apart vertically [6, 7]. Branches themselves in this case have a thickness from 150 to 300 nm. In this case there are lines in the irradiated nanocavity spherical diameter of from 10 nm to 20 nm. In this case irradiated structures have crystallographic symmetry of the initial structure.

We see two diffractive rings on Fig. 1(a) and Fig. 2(a). But really the number of diffractive rings may be more as two.

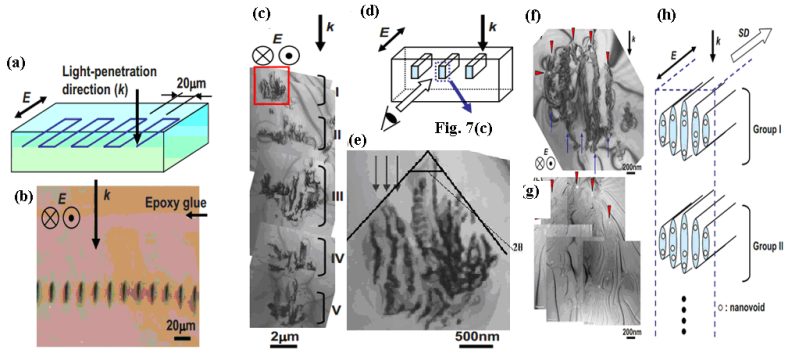

Fig7. *(a) Schematic illustration of the laser irradiated pattern. The light propagation direction (k) and electric field (E) are shown. (b) Optical micrograph of the mechanically thinned sample to show cross sections of laser-irradiated lines (200 nJ/pulse). (c) Bright-field TEM image of the cross section of a line written with pulse energy of 300 nJ/pulse. (d) Schematic illustration of a geometric relationship between the irradiated line and the cross-sectional micrograph. (e) Magnified image of a rectangular area in (c). Laser-modified layers with a spacing of 150 nm are indicated by arrows. (f) Bright-field TEM image of a portion of the cross section of a line written with a pulse energy of 200 nJ/pulse. (g) Zero-loss image of a same area as in (f) with nanovoids appearing as bright areas. Correspondence with (f) is found by noting the arrowheads in both micrographs. (h) Schematic illustrations of the microstructure of a laser modified line. Light-propagation direction (k), electric field (E), and scan direction (SD) are shown. Only two groups (groups I and II) of the laser-modified microstructure are drawn [6, 7].*

In this case diffraction processes may be generated in two stages: 1 – formation of diffraction rings of focused beams [2] and second – formation of diffracting gratings in the time of redistribution of second-order Cherenkov radiation [2 – 5]. Second case is analogous to the creation of self-diffraction gratings in NLO, but for Fig. 7 (c) and Fig. 7 (g) our gratings are limited by Much cone of Cherenkov radiation.

3. MODELING AND DISCUSSIONS

The first laser-induced filaments were received in the liquid. Later researches shown that analogous phenomena are generated in solid and gas matter too. Therefore first models were created for the nonlinear Kerr media and were used for all types of irradiated matter.

If the beam diameter is D, the beam might be expected to expand by diffraction with an angular divergence of $\theta = {1,22\lambda}/{n_0 D}$, where n_0 – linear refractive index of medium, λ – laser wavelength. Therefore Kerr media critical power may be determined as [11]

$$P_{cr} = (1.22\lambda)^2 \frac{c}{64 n_2}. \quad (1)$$

Where n_2 is nonlinear refractive index of the medium.

The self-focusing length determined with help next formula [11]

$$Z_{sf} = \frac{0.367 k \omega_0^2}{\left[\left(\sqrt{{P}/{P_{cr}}} - 0,852\right)^2 - 0,0219\right]^{1/2}}, \quad (2)$$

Where $k = {2\pi}/{\lambda}$ is the wave number, ω_0 – is the spot side of the pump beam, P – pump power.

This formula are using as basic for the determination of threshold self-focusing and self-trapping generation. But this formula can't be use for the determination threshold of power the optical breakdown. For example, the power of creation the laser filaments in irradiated matter may be ~700 *Pcr* [30]

In [21] formula for the determination P_{cr}, as threshold power of self-focusing, is represented in next form

$$P_{cr} = \frac{3.77\lambda^2}{8\pi n_0 n_2}. \quad (3)$$

Therefore first model were connected with self-focusing and self-trapping and liquid and other isotropic matter.

For Kerr media the change of refractive index is represented as $\delta n = K|E|^2$, where E is peak amplitude of linearly polarized field. According to [11] coefficient K have 12 presentations. But Kerr media are represented liquids basically. For solid state basic phenomena are laser-induced electrostriction [31]. In the gas case we can have other nonlinear optical phenomena. Therefore we must select more universal concept for the determination P_{cr}. It may be physical-chemical method. In this case we must have concentration of proper centers of scattering (absorption) of laser radiation, which are generated proper nonlinear optical phenomenon, and its activation energy. The self-focusing is nonlinear optical process therefore P_{cr} or the critical value of energy may be determined in next way. Volume density of energy of the creation self-focusing process may be determined with help next formula W_{crvol}

$$W_{crvol} = E_a N_{nc}, \quad (4)$$

where E_a – energy of activation proper "nonlinear" centers; N_{nc} – their concentration. Surface density for optical thin may be determined as

$$W_{crsur} = {W_{crvol}}/{\alpha}, \quad (5)$$

where α – absorbance index. Integral value of energy may be determined as

$$W_{crin} = W_{crsur} \cdot S, \quad (6)$$

where S – the square of irradiation.

In this case

$$P_{cr} = W_{crin} / \tau_{ir}, \quad (7)$$

where τ_{ir} is duration of laser irradiation.

The determination the concentration of scattering centers must be determined with conditions of proper experiment. It is determined by the conditions of observation the proper phenomena.

Next step of determination the density of energy in our cascade is condition of diffractive stratification. This condition may be determined with help of sizes the diffractive rings. We can estimate density of energy in plane of creation the diffractive stratification for n=5.

The explanation of creation the laser-induced filaments have various interpretation. Firstly [8] is the creation wave-guide zones after point of collapse [8]. In this case filaments have little life-time.

Conic part of filament radiation has continuum spectrum: from ultraviolet to infrared. At first this effect was called superbroadening. Therefore it may be interpreted as laser-induced Cherenkov radiation [2 – 5, 18]. The angle 2θ in the vertex of an angle of Fig. 7 (e) is double Cherenkov angle. In this case we have frozen picture of laser-induced destruction of 4H-SiC with help Cherenkov radiation.

The Cherenkov radiation is characterized by two peculiarities [32 – 35]: 1) creation of heterogeneous shock polarization of matter and, 2) radiation of this polarization. The methods of receiving shock polarization may be various: irradiation by electrons, γ-radiation, ions and excitation with help pulse fields. The stratification of this radiation on other type's radiation (volume, pseudo-Cherenkov a.o.) has relative character and may be represented as laser-induced Cherenkov radiation. Therefore in future we'll be represent conical part of filament radiation as Cherenkov.

This fact may be certified with macroscopic and microscopic ways.

First, macroscopic may be represented according to [18]. The similarity between charge particle and light-induced Cherenkov radiation one can invoke the analogy between Snell's law and Cherenkov radiation [18]. This natural since both effects can be derived in the same way from the Huygens interference principle. In Fig. 8(a) the point of intersection of a light pulse impinging at an angle φ on a boundary between two media moves with velocity $V = C / n_1 \cos\varphi$. This relation with Snell's law, gives the Cherenkov relation (Fig.8(a)).

$$\cos\theta = C / n_2(\omega) V. \quad (8)$$

This formula allows explain the angle differences for various type of Cherenkov radiation. In this case *V* may be represented as velocity of generation the optical-induced polarization too.

Thus the refraction law a light at the boundary between two media is the same as the condition for Cherenkov emission by a source moving along the boundary. In nonlinear medium the emitted frequencies may differ from the excitation frequency. The Cherenkov relation is still valid since the constructive interference occurs at a given Cherenkov angle for each Fourier frequency component of the light-induced nonlinear polarization. In a sense, one can speak about a nonlinear Snell-Cherenkov effect [18].

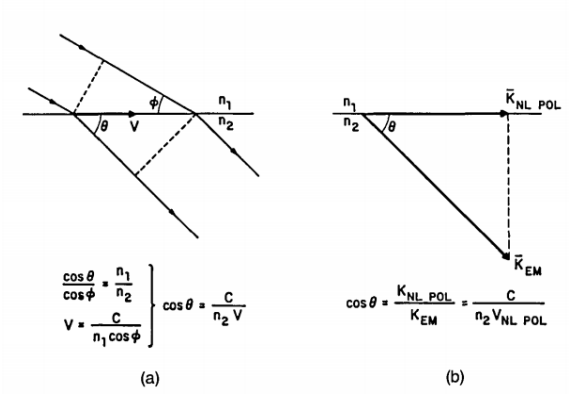

Fig8. [18]. *(a) Analogy between Snell's law and Cherenkov radiation. The point of intersection 0f a light pulse impinging upon a boundary two media moves with velocity* $V = \frac{C}{\cos\varphi}$. *Combining this relation w2ith Snell's law*

one obtains the Cherenkov relation, $\cos\theta = \frac{C}{n_2 V}$. *(b) The Cherenkov angle relation can be obtained from the conservation of the longitudinal component of a linear momentum at a boundary between to media along which a nonlinear polarization is propagated.*

The Cherenkov angle $\cos\theta = C/n_2(\omega)V$ can also be derived from the conservation of the longitudional component of of the linear momentum at a boundary between two media along which a nonlinear polarization is propagating (Fig. 8 (b)). Using $k = \omega/V$, we obtains

$$\cos\theta = k_{nl\ pol}(\omega)/k_{em}(\omega) = V_{em}/V_{nl\ pol} = C/n_2(\omega)V_{nl\ pol}. \quad (9)$$

The role of the boundary can be played by the surface of self-trapped filament. The nonlinear polarization propagating along this surface will result in a light-induced Cherenkov $\cos\theta = C/n_2(\omega)V$.

The nonconservation of the transverse component of the linear momentum can be related to the uncertainty principle, $\Delta x \Delta k > 1$, where Δx is the thickness of the boundary.

The microscopic mechanism of laser-induced Cherenkov radiation is expansion and application of Niels and Aage Bohrs microscopic theory of Cherenkov radiation as part of deceleration radiation on optical case [33]. For optical case the Bohrs hyperboloids must be changed on Gaussian distribution of light for mode TEM_{00} or distribution for focused light of laser beam [2 – 5]. In this case Cherenkov angle may be determined from next formula

$$\theta_{Ch} + \alpha_{ir} = \pi/4 \text{ or } \theta_{Ch} = \pi/4 - \alpha_{ir}, \quad (10)$$

where α_{ir} – angle between tangent line and direction of laser beam.

We can determine Cherenkov angles for data of Table 1. Angle α_{ir} was determined from next formula

$$\tan\alpha_{ir} = d_b/l_{sf}, \quad (11)$$

where d_b – diameter of laser beam, (7 mm), l_{sf} – length of self-focusing. In our case α_{ir} is angle of self-focusing.

This formula is approximate for average angle α_{ir}.

These data are represented in Table 3.

Table 3. *Self-focusing and Cherenkov angles for data of Table 1.*

	LiF	CaF_2	Fused silica	Water	BK7
α_{ir1}	49, 4	59	69,6	74	74
θ_{Ch1}	40,6	31	20,4	16	16
$n_2(\omega)V_{nl\ pol}, 10^3\ km/s$	394,8	349,7	319,9	311,9	311,9
α_{ir2}	75,6	79,3	82,5	84,1	84,3
θ_{Ch2}	14,4	10,7	7,5	5,9	5,7
$n_2(\omega)V_{nl\ pol}, 10^3\ km/s$	309,5	305,1	302,4	301,6	301,3

Remarks to Table 3. Index 1 for irradiation with $1{,}5\times10^{12}$ W/cm^2, index 2 for 1×10^{13} W/cm^2. Value of light velocity is 299792,458 *km/s*.

The Golub formula (8) was used in Table 3. We can determine product $n_2(\omega)V_{nl\ pol}$ uding this formula.

Thereby microscopic modified Bohrs theory and macroscopic Golum model are mutually complementary methods.

The decreasing of Cherenkov angle and product $n_2(\omega)V_{nl\ pol}$ for increasing of laser radiation intensity are corresponded to increasing of nonlinear refractive index and decreasing of velocity of polarization (multiphotonic and multiwave processes). In whole microscopic mechanism of laser-induced Cherenkov radiation may be represented as nonequilibrium spectrum of all possible Nonlinear Optical phenomena in the local points of propagation the laser beam. It may be Raman and Brillouin

scattering, up- and down-conversion, generation of harmonics and various interference of these processes and phenomena, which are generated the continuous spectrum from ultraviolet to infrared regions.

Cherenkov radiation with optical pumping may be represented as Nonlinear Optical process with velocity is less as light phase speed in irradiated matter. In this case phase speed in matter has physical nature: it is the electromagnetic speed of "collective" motion the charge particles or charge in matter. Therefore in local scale we have Nonlinear Optical processes, which are modulated of the Mach cone the Cherenkov radiation (Fig. 7 (c)). It allows add the Niels and Aage Bohrs theory about microscopic mechanism of Cherenkov radiation [40].

In solid this spectrum must be displaced to ultraviolet range? Therefore our traces of filaments have more little length as in water or air [13, 32]. Basis cause of this`` fact is more density of solid and more intensive light absorption. But in the liquid and air the direct optical breakdown is realized and these types of matter have more "soft" relaxation as solid. And processes of multiphoton ionization in the regime of self-focusing are more slowly as in solid. Continuum spectrum of filaments in this case are corresponded to the renewal disrupting chemical bonds and electronic states of irradiated molecules and atoms.

The estimation of sizes the cascade of volume destructions of Fig. 7 © may be explains in next way [2]. The sizes (diameters) of proper stages d_{nir} of cascade are proportionally to corresponding diffraction diameters d_{ndif}

$$d_{nir} = kd_{ndif}\,, \tag{12}$$

where k is the proportionality constant.

The diffraction diameters d_{ndif} may be determined with help condition of diffraction-pattern lobes (modified Rayleygh ratio)

$$d_{ndif} = n\lambda. \tag{13}$$

The estimations of diffraction diameters d_{ndif} for $\lambda = 800\ nm$ were represented in [2].

The distance between diffraction spots and proper moving foci may be determined with help next formula

$$l_{nf} = \frac{d_{ndif}}{2\tan \varphi/2}. \tag{14}$$

Where φ is focusing angle

These distances for $\varphi_1 = 20^o$ and $\varphi_2 = 30^o$ were represented in [2].

The conclusion about diffractive stratification of focused radiation may be certified by experimental data of Fig. 7 (c).

These results are corresponded to Lugovoy-Prokhorov theory too: distance between contiguous elements is smaller as distance between microscopy ocular and first stage of cascade (correlation of this distance is proportional to λ/d) [2] but distance between contiguous elements of cascade is equal and proportional to half wavelength.

Qualitative explanation of development of cascade the destructions may be next. The focus of each diffraction zone (spot) is the founder proper shock optical breakdown. But foci with more high number may placed in the "zone" of influence of previous foci. Therefore only first stage of Fig. 4 (c) is represented pure shock mechanism (Mach cone). Mach cones are characterized the second and third stages of Fig. 7 (c). But its maximums are displaced from center. It may be result if interaction second and third shock waves with previous shock waves: first – for second wave and first and second for third wave. The chock mechanism of destruction certifies a linear direction of optical breakdown. This direction is parallel to direction of shock wave and radiated spectrum is continuum as for Cherenkov radiation and as for observed laser-induced filaments in water and air [18, 19, 40]. Thus basic creator of optical breakdown traces is secondary Cherenkov radiation and shock waves. This

radiation is absorbed more effectively as laser radiation and therefore the creation of optical breakdown traces is more effectively as for beginning laser radiation. Cherenkov radiation is laid in self-absorption range of 4H-SiC, but 800 nm radiation – in intrinsic range. For the testing of this hypothesis we must measure the spectrum of secondary radiation. In this case we can use physical-chemical cascade model of excitation the proper chemical bonds of irradiated matter in the regime of saturation the excitation.

We can rough estimate basic peculiarities of energy distribution in Mach cone more precision formula as in [2 - 4]. This formula may be represented as

$$E_{1ob} = \frac{\pi^2}{4}\left(\sum_{i=1}^{5} n_{iav}^2 l_{iav}\right) r^2 N_{aSiC} E_{Zth}, \tag{15}$$

where n_{iav}– average visible number of filaments in proper group of cascade, l_{iav}=1000 *nm* – average length of filaments in proper group of cascade, r = 10 nm – average radius of filament, N_a – atom density of 4H-SiC, $E_{Zth} \sim 25\ eV$ – Zeitz threshold energy for 4H-SiC.

The atom density of 4H-SiC may be determined with help next formula

$$N_a = \frac{n\rho N_A}{A}, \tag{16}$$

where ρ – density of semiconductor, N_A – Avogadro number, A – a weight of one gram-molecule, n – number of atoms in molecule. For 4H-SiC $N_{aSiC} = 9,4 \cdot 10^{21}\ cm^{-3}$.

For further estimation we use next approximation $n_{1av} = n_{2av} = n_{3av} = n_{4av} = n_{5av} = 100,$ (see Fig. 7 (c)).

Energy, which is necessary for the optical breakdown our nanotubes may be determined in next way. Zeitz threshold energy for 4H-SiC is equaled $E_{Zth} \sim 25\ eV$. Let this value is corresponded to energy of optical breakdown. Therefore summary energy E_{1ob} is equaled

$$E_{1ob} = N_{asnt} \cdot E_{Zth} = 23,2\ nJ. \tag{17}$$

This value is equaled of ~ 8% from pulse energy or ~ 30% from the effective absorbed energy of pulse. In this case we have more high efficiency of transformation initial radiation to "irreversible" part of Cherenkov radiation. It is result of more intensive excitation comparatively with classical methods of receiving the Cherenkov radiation. In this case we have pure photochemical processes. The experimental data for intrinsic absorption (Fig. 7) show that for short pulse regime of irradiation (femtosecond regime) basic processes of destruction the fused silica and calcium fluoride are photochemical (multiphoton absorption in the regime of saturation the excitation). But basic peculiarity of experimental data Fig.7 is transformation the initial laser radiation (wavelength 800 *nm*) to continuum Cherenkov radiation. From length of optical breakdown in 4Y-SiC we can determine average absorption index of Cherenkov radiation. It is ~ 10^4 cm^{-1}. This value is corresponded to violet-blue range of absorption spectrum of 4H-SiC. It is corresponded to ultraviolet and violet range of absorption spectrum of 4H-SiC [2].

We can estimate chain of critical value of energy for the 4*H-SiC* from physical-chemical point of view too.

Critical value of energy, which is necessary for the beginning of self-focusing, may be determine in next way. Volume density of energy of the creation self-focusing process may be determined with help formula (4). In further we made next approximation: $E_a = h\nu = 1,5\ eV$; $N_{nc} = \left(10^{14} - 10^{16}\right) cm^{-3}$. Then we have for SiC $W_{crvol} = 2,4 \cdot \left(10^{-5} - 10^{-3}\right) J/cm^3$. `For *SiC* α = 0,1 cm^{-1}. And $W_{crsur} = 2,4 \cdot \left(10^{-4} - 10^{-2}\right) J/cm^2$.

Integral value of energy may be determined according by formula (6). For Fig. 7(c) for r = 2 μm, S = $1,256 \cdot 10^{-7}\ cm^2$. Therefore $W_{crin} = 3\left(10^{-11} - 10^{-9}\right) J$. For r = 1 *mm* we have $W_{crin} = 1,9\left(10^{-6} - 10^{-4}\right) J$.

These estimations are corresponded to estimations, which are received with help formulas (1), (3) and other, simple to its [11], electrodynamic formulas. For the gases this method allows to estimate the energy of its optical breakdown.

Next step of determination the density of energy in our cascade is condition of diffractive stratification. This condition may be determined with help of sizes the diffractive rings. We can estimate density of energy in plane of creation the diffractive stratification for n=5.

Maximum diameter of diffractive pattern is determined for fifth diffractive ring. For this case average density of energy in plane of diffractive rings is equaled

$$W_{avdr} = E_p \Big/ S . \qquad (18)$$

Where E_p – energy of laser pulse. For E_p = 200 nJ and E_p = 300 nJ and S =1,256·10^{-7} cm^2 we have next value of W_{avdr} 1,6 J/cm^2 and 2,4 J/cm^2. If we multiple these value of the absorbance index of SiC α = 0,1 cm^{-1} then we are receiving the volume density of energy $W_{avdrvol}$ 0,16 J/cm^3 and 0,24 J/cm^3. Really value is 0,4 from represented data (reflectance is 0,6) and are 0,064 and 0,096 J/cm^3

Correlation $W_{avdrvol}/W_{crvol}$ for real values for SiC is equaled from 27 to 2700.

Density of energy of optical breakdown W_{ob} for SiC is equaled 18800 J/cm^3. Therefore correlation $W_{ob}/W_{avdrvol}$ is equaled 78333 and 117500.

The analogous chain processes may be mage for other media. Density $W_{avdrvol}$ was determined for the five diffractive rings. Results of these estimations are represented in Table 4. The results of Table 1 and table 2 and [19] were used for the formation the data of Table 4.

Table 4. *Energetic chain for the corresponding processes in some media.*

media	N_a, cm^{-3}	λ_{ir}, nm	τ_{ir}	E_p	W_{crvol}, J/cm^3	$W_{avdrvol}$, J/cm^2	W_{ob}, J/cm^3
4H-SiC	$9,4\cdot10^{21}$	800	130 fs	300 nJ	$2,4\cdot\left(10^{-5}-10^{-3}\right)$	1,6; 2,4	18800
LiF	$1,2\cdot10^{22}$	796	140 fs	$1,3J/cm^2$	$2,4\cdot\left(10^{-5}-10^{-3}\right)$	9,57	24000
LiF	$1,2\cdot10^{22}$	393	100 fs	$0,15J/cm^2$	$4,8\cdot\left(10^{-5}-10^{-3}\right)$	3,75	24000
Water	$1,0\cdot10^{22}$	796	140 fs	$0,62J/cm^2$	$2,4\cdot\left(10^{-5}-10^{-3}\right)$	3,76	4000
Water	$1,0\cdot10^{22}$	393	100 fs	$0,15J/cm^2$	$4,8\cdot\left(10^{-5}-10^{-3}\right)$	3,75	4000
CaF_2	$7,6\cdot10^{21}$	796	140 fs	$1,0J/cm^2$	$2,4\cdot\left(10^{-5}-10^{-3}\right)$	6,82	15200
CaF_2	$7,6\cdot10^{21}$	393	100 fs	$0,15J/cm^2$	$4,8\cdot\left(10^{-5}-10^{-3}\right)$	3,75	15200
D_2O	$1,0\cdot10^{22}$	796	140 fs	$0,46J/cm^2$	$2,3\cdot\left(10^{-5}-10^{-3}\right)$	3,26	3800
D_2O	$1,0\cdot10^{22}$	530	15 ps	$15J/cm^2$	$2,3\cdot\left(10^{-5}-10^{-3}\right)$	240	3800
NaCl	$4,4\cdot10^{21}$	796	140 fs	$0,29J/cm^2$	$2,4\cdot\left(10^{-5}-10^{-3}\right)$	0,72	8800
fused silica	$1,3\cdot10^{22}$	796	140 fs	$0,57J/cm^2$	$2,4\cdot\left(10^{-5}-10^{-3}\right)$	3,89	26000
CS_2	$3,0\cdot10^{21}$	796	140 fs	$0,01J/cm^2$	$2,4\cdot\left(10^{-5}-10^{-3}\right)$	0,15	6000
CCl_4	$3,1\cdot10^{21}$	796	140 fs	$0,44J/cm^2$	$2,4\cdot\left(10^{-5}-10^{-3}\right)$	2,10	6200
C_2HCl_3	$4,1\cdot10^{21}$	796	140 fs	$0,08J/cm^2$	$2,4\cdot\left(10^{-5}-10^{-3}\right)$	1,08	8200

We must make some remarks to Table 4. Density of energy the optical breakdown of water is 495 kJ/mol or 2,5 $eV/atom$. Therefore for liquids this quantity is less as for solid. Threshold critical values of volume density of energy for self-focusing are quantities with almost equivalents values. Therefore these values lay in the region $m\cdot\left(10^{-5}-10^{-3}\right)J/cm^3$, where $m\in[2,3;4,8]$.

For the gases real regimes of irradiation are similar to regime of optical breakdown. Therefore the chain of corresponding processes may be differ from solid and liquid case.

But experimental data of Fig 5 may be explained analogously to 4H-SiC. But in this case we have two diffractive rings. Cherenkov angle is equaled ~1''. Therefore interference of Cherenkov radiation is

realized on distance 30 m from peak of Cherenkov angle. Phase conditions of realization of this interference are stronger as for 4H-SiC.

Concept of diffractive stratification allows explaining the surface character of Cherenkov radiation. This radiation is generated in the region of proper focused diffractive ring [2].

The data of Fig. 6 is analogous to Rustamov-Pilipetskiy data [17]. But in this case we have temporal dynamic of interaction laser radiation and liquid. Fig. 6(b) is dynamic evolution map of first 30% of initial map of Fig. 6 (a).

The questions about supercontinuum radiation in the process of femtosecond laser filamentation are discussed in [11 – 13]. In air supercontinuum spectra laid from ultraviolet to infrared ranges of spectra. In whole nonlinear optics of filaments is included the superexpansion of frequency-angle spectrum of initial pulse, generation of more higher harmonics and terahertz irradiation, pulse compression, optical anisotropy of filament and other nonlinear phenomena [1, 32].

But only shock processes (heterogeneous laser-induced polarization of irradiated matter) can explain of represented experimental data.

Experimental data of Fig. 7 may be explain on the basis the two-dimensional interference of various waves or polariton-plasmon according by V. Makin [36]. Maxima of these interferograms are sources of more intensive ionization of irradiated matter and concomitant processes of phase transformations (Fig. 7) or radiation (Fig. 5).

The sizes of nanovoids (Fig. 7 (h)) may be determined with help modified Rayleygh model [2 – 4] and its form – the help methods of continuum mechanics [2 – 4].

As we see sources of Relaxed Optical processes are Optical and Nonlinear Optical processes and phenomena.

4. Conclusion

1. The experimental data of creation laser-induced filaments in various media (solid, liquid and gas) are represented and analyzed as Nonlinear and Relaxed Optical processes and phenomena.
2. The chain of possible processes are represented and modeled.
3. The question about correlation between nonequilibrium and irreversible processes and phenomena are represented.
4. Microscopic (modified Bohrs model) and macroscopic aspects (Golub model) of laser-induced Cherenkov radiation are analyzed.
5. The role the Cherenkov radiation and its interference on the formation microscopic stratification filaments is observed.
6. The bond between parameters of focusing, including self-focusing, of laser-radiation, Cherenkov angle, nonlinear refractive index and velocity of polarization the irradiated matter are represented and discussed.
7. Peculiarities of generation and evolution of laser-induced filaments in various media are analyzed.
8. Various models of stratification the laser radiation and laser-induced structures are represented and discussed.

References

[1] Manenkov A. A., Prokhorov A. M. (1986) Laser destruction of transparent solid. Advanced in physical science. Vol. 148, Is. 1, 179-211 (In Russian)

[2] Trokhimchuck, P. P. (2019) Problems of modeling diffraction and interference processes in Nonlinear and Relaxed Optics. IJARPS. Vol. 6, Is. 7, 5-17

[3] Trokhimchuck P. P. (2018) Problems of modeling the phase transformations in Nonlinear and Relaxed Optics (review). IJERD. Vol.14, Is.2, 48-61

[4] Trokhimchuck P. P. (2018) Some Problems of Modeling the Volume Processes of Relaxed Optics. IJARPS. 2018. Vol. 5. Is. 11, 1-14

[5] Trokhimchuck P. P. (2016) Relaxed Optics: Realities and Perspectives. Lambert Academic Publishing, Saarbrukken

[6] Okada T., Tomita T., Matsuo S., Hashimoto S., Ishida Y., Kiyama S., Takahashi T. (2009) Formation of periodic strain layers associated with nanovoids inside a silicon carbide single crystal induced by femtosecond laser irradiation. J. Appl. Phys., Vol. 106, p. 054307, – 5 p.`

[7] Okada T., Tomita T., Matsuo S., Hashimoto S., Kashino R., Ito T. (2012) Formation of nanovoids in femtosecond laser irradiated single crystal silicon carbide. Material Science Forum, Vol. 725, 19 – 22

[8] Self-Focusing: Past and Present. (2009) Springer Series: Topics in Applied Physics. Vol. 114. Eds. R. W. Boyd, S. G. Lukishova, Y.-R. Shen. Springer Verlag, NY

[9] Bloembergen N. (1973) The influence of electron plasma formation on superbroadening in light filaments. Opt. Commun. Vol.8, Is. 4, 285-288.

[10] Akhmanov S. V., Sukhorukov A.P., Khohlov R. V. (1967) Self-focusing and diffraction of light in Nonlinear media. Advanced in physical science. Vol. 93, Is. 1, 19-70 (In Russian)

[11] Marburger J. H. (1975) Self-focusing: theory. Progr. Quant. Electr. Vol. 4, 35-110

[12] Trokhimchuck P. P. (2019) Problem of modeling the filaments for laser-induced breakdown of matter. Proc. of XII Int. Conf. "Quantum Electrronics", Minsk, Belorussian State University, November 18-22, 2019, 37- 39 (In Russian)

[13] Trokhimchuck P. P. Problems of reradiation and reabsorption in Relaxed Optics. IJARPS. 2017. Vol. 4, Is. 2, 37 – 50

[14] Chekalin S. V., Kandidov V. P. (2013) From self-focusing light beams to femtosecond laser pulse filamentation. Advanced in physical science. Vol. 56, Is. 2, 123-140 (In Russian)

[15] Trokhimchuck P. P. (2019) Cherenkov Radiation and Relaxed Optics. Proc. of the 13-th Int. Conf. "Interaction of Radiation with Solids", Minsk, Belarus, September 30 – October 3, 2019, 30-32

[16] Trokhimchuck P. P. (2019) Problems of modeling the Cherenkov radiation and shock processes in Relaxed Optics. / Proc. IV Int. Conf "Optics of heterogeneous media", Arkadiy Kuleshov Mogilev State University. May 28-29, 2019, 3-9

[17] Pilipetskiy N. F., Rustamov A. R. (1965) Observation of light self-focusing in liquids. JETP Letters. Vol. 2, Is.2, 88 – 90 (In Russian)

[18] Golub I. (1990) Optical characteristics of supercontinuum generation. Optics Letters. Vol. 15, Is.6, 305-307

[19] Golub I., Shuker R., Eres G. (1986) On the optical characteristics of the conical emission.// Optics Communications. Vol. 57, Is. 2, 143-145

[20] Nagura C., Suda A., Kawano H., Obara M., Midorikawa K. (2002) Generation and characterization of ultrafast white-light continuum in condensed media. Appl. Opt. Vol. 41, Is. 18, 3735-3742

[21] Shen J. (1987) Principles of Nonlinear Optics. Nauka, Moscow (In Russian)

[22] Minardi S., Gopal A., Tatarakis M., Couairon A., Tamosăuskas G., Piskarskas R., Dubietis A., Di Trapani P. (2008) Time-resolved refractive index and absorption mapping of light-plasma filaments in water. Opt. Lett. Vol.33, Is. 1, 86-88

[23] Vaichaitis V. I., Ignavichyus M. V., Kudryashov V. A., Pimenov V. N. Observation of a Cherenkov type radiation during the propagation of picosecond light pulse in sodium vapor. JETP Letters. Vol. 45, Is. 7, 414-417

[24] Nishioka H., Odajima W., Ueda K., Takuma H. (1995) Ultrabroadband flat continuum generation in multichannel propagation of terawatt Ti:sapphire laser pulses. Opt. Lett. Vol. 20, Is. 24, 2505-2507.

[25] Corcum P. B., Rolland C., Shrivasan-Rao T. (1986) Supercontinuum generation in gases. Phys. Rev. Lett. Vol. 57, Is. 18, 2268-2271

[26] Lugovoy V. N., Prokhorov A. M. (1973) Theory of propagation of power laser radiation in nonlinear media. Advanced in physical science. Vol. 11, Is. 2, 203 – 247 (In Russian)

[27] Smith W. L., Liu P., Bloembergen N. (1977) Superbroadening in H_2O and D_2O by a self-focused picosecond pulse YAlG:Nd laser. Phys. Rev. A. Vol. 15, Is. 6, 1977, 2396-2403.

[28] Ivanisik A. I., Isayenko A. Yu., Korotkov P. A., Ponezha G. V. (2012) Phase-modulated parametric anti-Stokes stimulated Brillouin scattering of Cherenkov type in the region of self-focusing excited radiation. Ukr. Phys. Joornal. Vol. 57, Is.10, 1000-1010 (In Ukrainian)

[29] Brodeur A., Chin S. L. (1998) Band-gap dependence of the ultrafast white-light continuum.// Phys. Rev. Lett. Vol. 80, Is. 20, 4406-4409

[30] Berge L., Skupin S., Lederer F., Mejean G., Yu J., Kasparian J., Salmon E., Wolf J. P., Rodrigues M., Wöste L., Bourayou R. and Saurbrey R. (2004) Multiple Filamentation of Terawatt Laser in Laser, Phys. Rev. Lett. Vol. 92, Is. 22, p. 225002, 4 p.

[31] Sharma B. S. (1968)Laser-induced dielectric breakdown and mechanical damage in silicate glasses. Ph. D. Thesis. Simon Fraser University, Burnaby

[32] Frank I. M. (1988) Cherenkov Radiation. Theoretical Aspects, Nauka, Moscow (In Russian).

[33] Bohr N. (1950) The passage of charged particles through matter. IL, Moscow (In Russian)

[34] Konkov A. S. (2015) Characteristics of polarized radiation the charged particles and magnetic moments. Ph. D. Thesis. Polytechnical university, Tomsk (In Russian)

[35] Bolotovskiy B. M., Ginzburg V. L. (1972) Vavilov-Cherenkov and Doppler effects in the time the motion of sources with speed greater as light speed in vacuum. Advanced in physical science. Vol. 106, Is. 4, 577-592 (In Russian)

[36] Makin V. S. (2013) Peculiarities of the formation the ordered micro and nanostructures in condensed matter after laser excitation of surface polaritons modes. D. Sc. Thesis. State university of information technologies, mechanics and optics, Saint-Petersburg (In Russian)

Citation: *Petro P. Trokhimchuck, (2020). "Some Problems of Modeling Laser-Induced Filaments: Nonlinear and Relaxed Optical Aspects". International Journal of Advanced Research in Physical Science (IJARPS) 7(2), pp.1-15, 2020.*